ACS OMEGA

Open Access

http://pubs.acs.org/journal/acsodf

Article

Caftaric Acid Ameliorates Oxidative Stress, Inflammation, and Bladder Overactivity in Rats Having Interstitial Cystitis: An In Silico Study

Saima, Irfan Anjum,* Saima Najm, Kashif Barkat, Hiba-Allah Nafidi, Yousef A. Bin Jardan, and Mohammed Bourhia

Cite This: *ACS Omega* 2023, 8, 28196−28206

Read Online

ACCESS | Metrics & More | Article Recommendations

ABSTRACT: Interstitial cystitis (IC) is the principal unwanted effect associated with the use of cyclophosphamide (CYP). It results in increased oxidative stress, overexpression of proinflammatory cytokines, and bladder overactivity. Patients receiving CYP treatment had severely depreciated quality of life, as the treatment available is not safe and effective. The goal of this study was to assess the protective effect of caftaric acid in CYP-induced IC. IC was induced in female Sprague Dawley by injecting CYP (150 mg/kg, i.p.). In the present study, oral administration of caftaric acid (20, 40, and 60 mg/kg) significantly decreased inflammation. Caftaric acid significantly increased SOD (93%), CAT (92%), and GSH (90%) while decreased iNOS (97%), IL-6 (90%), TGF 1-β (83%), and TNF-α (96%) compared to the diseased. DPPH assay showed the antioxidant capacity comparable to ascorbic acid. Molecular docking of caftaric acid with selected protein targets further confirmed its antioxidant and anti-inflammatory activities. The cyclophosphamide-induced bladder overactivity had been decreased possibly through the inhibition of M_3 receptors, ATP-sensitive potassium channels, calcium channels, and COX enzyme by caftaric acid. Therefore, our findings demonstrate that caftaric acid has a considerable protective role against CYP-induced IC by decreasing the oxidative stress, inflammation, and bladder smooth muscle hyperexcitability. Thus, caftaric acid signifies a likely adjuvant agent in CYP-based chemotherapy treatments.

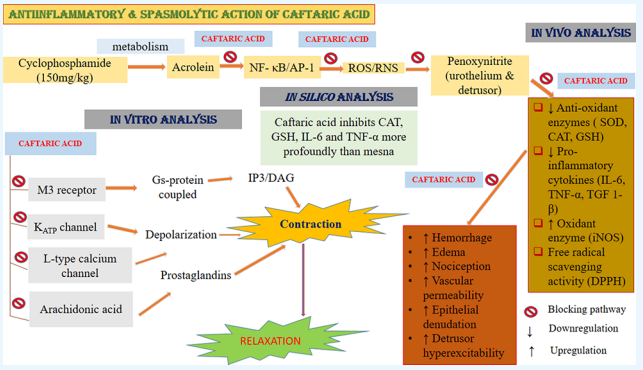

1. INTRODUCTION

Interstitial cystitis (IC) is a chronic disease characterized by pain in lower abdominal areas associated to filling of bladder, urgency, increased urinary rate, and nocturia. Females are affected more than males. The projected ratio of female to male is 5:1.[1] Its pathophysiology is not completely understood. The glycosaminoglycan (GAG) layer of the urothelium might be destructed and hence the toxic components are excreted in urine.[2] Cyclophosphamide (CYP) is an alkylating agent used in the treatment of many cancer conditions. Hemorrhagic cystitis is the major adverse effect of CYP.[3] Acrolein is the metabolite of CYP; it accumulates in the bladder, leading to the production of reactive oxygen species (ROS) and nitric oxide (NO) via direct and indirect mechanisms through the transcription of nuclear factor-κB (NF-κB) and activator protein-1 (AP-1). ROS and NO raise the levels of peroxynitrite in urothelium and detrusor. It causes cell necrosis and damages DNA, peroxidation of lipids, and oxidation of proteins. This then diminishes reduced glutathione (GSH), catalase (CAT), and superoxide dismutase (SOD) while increases the production of proinflammatory cytokines, interleukin-6 (IL-6), tissue necrosis factor-α (TNF-α), and transforming growth factor 1-β (TGF 1-β).[4−6] Edema, hemorrhage, urothelial ulceration, lymphocyte infiltration, and detrusor smooth muscle overactivity are associated with CYP administration.[7]

Cytokines play a crucial role in the pathogenesis of IC. Interleukins secreted locally from ulcerated urothelia attract immune cells that contribute to the development of pathological changes in bladder. IL-6 and TNF-α stimulate nociceptive nerves, while TGF 1-β causes vasodilation and edema through the mast cell infiltration.[8,9] Detrusor hyperexcitability was related to IL-6 secretion manifested by the

Received: March 13, 2023
Accepted: July 12, 2023
Published: July 25, 2023

increase in urine frequency and decrease in urine volume per void. ROS and cytokine turnover maintain an inflamed environment. Generation of free radicals also plays a part in the inflammatory process. GSH, CAT, and SOD protect the cells from free radicals as they have the ability to scavenge them. Free radicals could destroy the cell and its components. Bladder inflammation is linked with the increased secretion of cytokines and the decrease of antioxidant defense.[1] Muscarinic receptors are abundantly found in bladder tissue. The cholinergic responses are altered in inflammatory state.[10] Detrusor overactivity is reported in cystitis.[7]

Mesna is the only prescribed drug to prevent CYP-associated interstitial cystitis. It binds with acrolein, thus preventing its deleterious responses.[11] It however is not capable of completely reverting interstitial cystitis.[12] Many studies favor the use of phytochemicals with antioxidant potential to be safe alternatives to mesna.[11]

Alternative medicine has gained immense attention for treating a variety of pathological conditions. Herbal extracts are the rich sources of antioxidants and anti-inflammatory substances.[13] Many phytochemicals are analyzed for their role in treating cyclophosphamide-induced interstitial cystitis and proved effective.[14]

Caftaric acid (caffeoyltartaric acid) is a chief phenol found in grapefruit juice, lettuce, spinach, and wine.[15,16] It has free hydroxyl groups that have oxidant-lowering capacity.[16] It successfully resolves gastric ulcer induced by indomethacin in rats.[17] Its role in the treatment of interstitial cystitis has not been studied yet. The present study aimed to determine the uroprotective role of caftaric acid in CYP-induced interstitial cystitis.

2. MATERIALS AND METHODS

2.1. Chemicals Used. All chemicals used during the study were of analytical grade. These include cyclophosphamide, mesna, atropine, glibenclamide, indomethacin, propranolol, 4-diphenylacetoxy-*N*-methylpiperidine (4-DAMP), methoctramine, barium chloride, nifedipine, carbachol, potassium dihydrogen phosphate (KH_2PO_4), potassium chloride (KCl), sodium chloride (NaCl), sodium bicarbonate ($NaHCO_3$), calcium chloride ($CaCl_2$), glucose monohydrate ($C_6H_{12}O_6$ H_2O), DPPH (1,1-diphenyl-picrylhydrazyl), and magnesium sulfate ($MgSO_4$), which were obtained from Sigma Chemical Company. Cyclophosphamide was reconstituted in sterile normal saline to make an injectable solution. Caftaric acid (99%) was purchased from Na-Ha Nutri China and reconstituted in 0.5% carboxymethylcellulose sodium (CMC Na) for oral gavage and in methanol for the experiment on isolated rat bladder strips. Krebs−Henseleit solution was prepared freshly in distilled water every time before use. The dilutions of atropine, nifedipine, and indomethacin were prepared in ethanol; propranolol, methoctramine, carbachol, and barium chloride in distilled water; glibenclamide in DMF (dimethylformamide); and 4-diphenylacetoxy-*N*-methylpiperidine (4 DAMP) in DMSO (dimethylsulfoxide). All the dilutions were prepared freshly before use.

2.2. Animals Used. The study was conducted on female Sprague−Dawley rats weighing 200−250 g. They were retained in Animal House of Faculty of Pharmacy, The University of Lahore, Lahore, in a controlled environment of temperature (21 ± 3 °C), relative humidity (60 ± 5%), and 12 h light/dark cycles with free access to standard food and water ad libitum. Before starting the study, the animals were acclimatized for a duration of 1 week. All experimental procedures were approved and commenced under Institutional Research and Ethical Committee of Faculty of Pharmacy (IREC-2022-05), The University of Lahore, Lahore, Pakistan.

2.3. Cyclophosphamide-Induced Interstitial Cystitis. After acclimation, the female rats were injected CYP at a dose of 150 mg/kg body weight to induce interstitial cystitis on days 1, 4, and 7, respectively. Normal saline was injected to control animals of the same volume as a substitute of cyclophosphamide, following the same protocol. The animals were sacrificed on 8th day. The bladder of saline- and cyclophosphamide-treated rats were excised immediately to be used in the study.[18]

2.4. Study Design. All the rats were allocated randomly to six groups ($n = 3 - 6$). Control: received normal saline (0.9% NaCl) on days 1, 4, and 7 through the intraperitoneal route (IP). Diseased: CYP (150 mg/kg) was injected on days 1, 4, and 7 through the intraperitoneal route. Mesna (40 mg/kg) was given orally 1 h ahead of CYP injection on days 1, 4, and 7. Caftaric acid-treated (20, 40 and 60 mg/kg): it was administered orally 1 h before injecting CYP through the IP route on days 1, 4, and 7, respectively.

2.5. Quantitative Real-Time PCR Analysis. From the urinary bladder cells, the total RNA was isolated with the trizol (TRI) reagent (Sigma Chemical Company) according to the manufacturer's instructions. The complementary DNA (cDNA) was synthesized by using a WizScript cDNA synthesis kit (Wizbio Solutions, New Mexico, USA). To perform quantitative polymerase chain reaction, SYBR Green qPCR mix (Zokeyo, Wuhan, China) was employed. The relative transcription of target genes was determined by the $2^{-\Delta\Delta Ct}$ method using hypoxanthine−guanine phosphoribosyltransferase (HRPT) as an internal control reference gene.[19,20]

2.6. Assessment of Nociception. Before conducting the study, all animals were acclimatized for half an hour. They were then observed for a change in behavior after receiving the last dose of CYP in an open field study.[21] The locomotor activity index was measured by placing each rat in an observation box divided into nine squares. For 10 min, the number of boxes crossed by each rat with four paws was counted.[22]

2.7. Edema and Hemorrhage. Upon execution, the bladder of the animal was removed. It was weighed, and the weight was expressed in mg.[14] An increase in the bladder wet weight indicates the presence of edema. Both edema and hemorrhage were determined according to Gray's criteria.[21]

2.8. Vascular Protein Leakage Test. Evans blue dye (25 mg/kg) was given through the infusion route to the animal along with the last dose of CYP half an hour before execution. The rats were executed to isolate the bladder. To each bladder, 1 mL of formamide was added and incubated overnight at 56 °C. The extracted dye concentration was measured by calculating absorbance at 600 nm and comparing it to the standard Evans blue dye (μg/bladder).[23]

2.9. Antioxidant Analysis. The antioxidant capacity of caftaric acid was analyzed by 1,1-diphenyl-picrylhydrazyl radical (DPPH) free-radical scavenging assay. DPPH (0.2 mM) was prepared in aqueous methanol (80%). Caftaric acid solution was prepared in methanol (35 mg/mL) and diluted serially to obtain 30, 25, 20, 15, 10, and 5 mg/mL respectively. Ascorbic acid (Vitamin C) was utilized as the standard. The control solution did not contain caftaric acid. Freshly prepared 2 mL of DPPH solution was added to 2 mL of sample. They were mixed and incubated in dark at 37 °C for 30 min. The

https://doi.org/10.1021/acsomega.3c01450
ACS Omega 2023, 8, 28196−28206

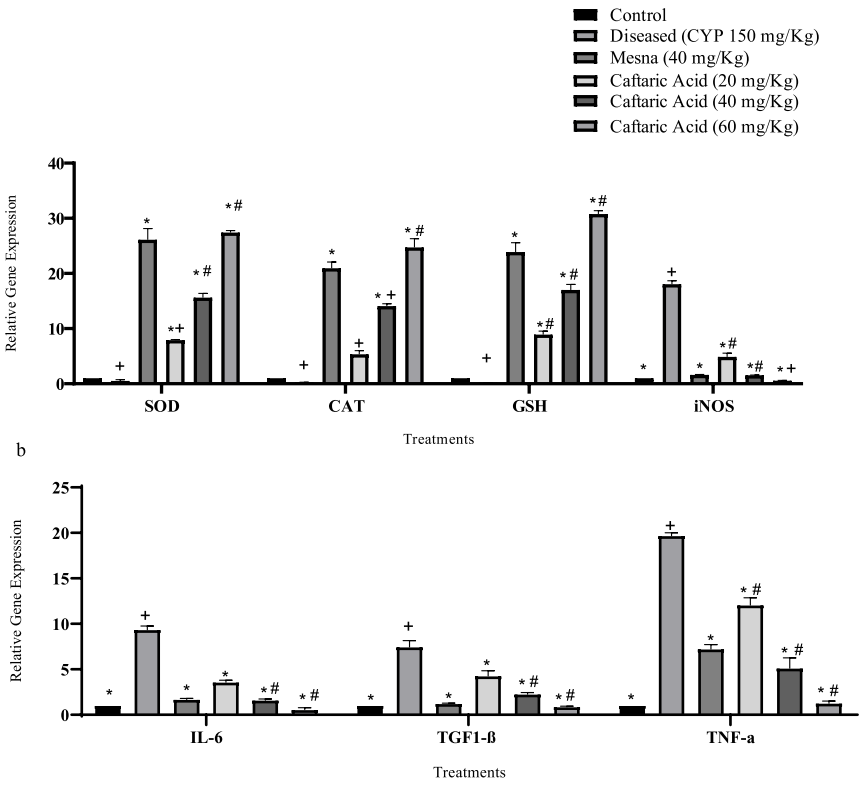

Figure 1. Reverse transcription polymerase chain reaction of the oxidant, antioxidant enzymes, and cytokines. (a) Relative gene expression of superoxide dismutase (SOD), catalase (CAT), glutathione reductase (GSH), and inducible nitric oxide synthase (iNOS). (b) Interleukin-6 (IL-6), transforming growth factor 1-β (TGF 1-β), and tissue necrosis factor-α (TNF-α) mRNA as normalized to hypoxanthine−guanine phosphoribosyltransferase (HPRT) mRNA. The values were expressed as mean ± standard error of mean; n = 3. $^{*}P < 0.05$, significant compared to the diseased control group. $^{+}P < 0.05$, significant compared to mesna and $^{\#}P < 0.05$, nonsignificant compared to mesna. Two-way ANOVA, followed by Tukey's multiple comparison test. Vertical bars represent SEM.

absorbance was measured at 517 nm against blank using a UV/vis HALO SB-10 spectrophotometer. The percentage free-radical scavenging capacity (% RSC) was determined by the following formula

$$\%\mathrm{RSC} = \left(\frac{\text{absorbance of control} - \text{absorbance of sample}}{\text{absorbance of controls}}\right) \times 100$$

where the absorbance of the control is the absorbance of DPPH and the absorbance of the sample is the absorbance of the test sample.[24,25]

2.10. Histological Analysis. The sections of bladder were preserved in formalin solution (10%). These were stained with hematoxylin−eosin (H&E) and periodic acid-Schiff (PAS) staining using the routine protocol. Edema, leukocyte infiltration, and urothelium damage were determined by H&E staining, while PAS staining determined glycosaminoglycan.[26,27]

2.11. Molecular Docking Analysis. *2.11.1. Ligand Selection.* To explore the uroprotective effect of the drug, ligand coordination spheres were prepared. The two-dimensional structure of caftaric acid (caf) (https://pubchem.ncbi.nlm.nih.gov/compound/Caftaric-acid/6440397) and mesna (mes) (https://pubchem.ncbi.nlm.nih.gov/compound/29769) were acquired from the PubChem database in SDF file format and changed to PDB format by the Open Babel GUI 3.0 software.[28] Then, the PDB file of ligands was utilized for automatic docking at several receptors by Auto Dock Tools software.[29]

2.11.2. Characterization of Receptors. The crystal structures of catalase (CAT), glutathione (GSH), and proinflammatory cytokines (IL-6 and TNF-α) were acquired from RCSB Protein Data Bank (PDB), with PDB ID: 1DGB (https://www.rcsb.org/structure/1dgb) for CAT; PDB ID: 3DK4 (https://www.rcsb.org/structure/3dk4) for GSH; PDB ID: 4ZS7 (https://www.rcsb.org/structure/4zs7) for IL-6; and PDB ID: 4TWT (https://www.rcsb.org/structure/4twt) for TNF. By means of Auto Dock Tools 1.5.6, the crystal structures of numerous receptors were modeled and purified. Then, polar hydrogen and partial charges were added. For analysis, interactions with the respective ligand macromolecules were saved in the relevant PDBQT format.[30] The most prominent active region of the enzyme along with the residues of amino acids was selected by pointing to the binding site involving ligand binding.[31]

2.11.3. Docking Studies. The ligand protein interactions were projected through docking.[32] In this study, mesna (mes) was assigned as the standard drug at various receptors for uroprotective potential. Computational designing of the drug offered the platform to comprehend the ligand−receptor connections.[33] Receptor scoring and docking were calculated by Auto Dock Tools 1.5.6 software; it mimics the binding conformations of ligands to exploit the binding sites of the docked molecule that uses Lamarckian genetic algorithm (LGA). The grid box was fixed at 70 × 70 × 70 Å alongside X, Y, and Z axes using the following auto dock parameters: 1.

https://doi.org/10.1021/acsomega.3c01450
ACS Omega 2023, 8, 28196−28206

Genetic algorithm per population size = 150; 2. Maximum number of energy evaluations = 2,500,000; 3. Crossover- mode genetic algorithm = 2 points. For the receptor, the parameters for rigidity were set keeping the ligand flexible. The chemical properties and structure of active sites enable binding and ligand recognition. From the ligand− protein interactions, 10 docked conformations (poses) were obtained. From the numerous binding interactions, the best conformation was assessed in terms of the least binding energy. They were additionally explored using PyMOL molecular graphics system offline software, along with online structure-based modeling servers like protein−ligand interaction profiler (PLIP) and Zentrum protein plus. The model was then validated.[29]

2.12. In Vitro Activity on Isolated Rat Bladder Strips. The bladders of both the control and CYP-treated rats were surgically removed upon execution. Each bladder was cut longitudinally to obtain four strips. It was immersed in 20 mL of Krebs−Henseleit solution at 37 °C pumped with carbogen in a tissue organ bath. The tissue was given initial 1 g tension and equilibrated for 1 h to retain it. The viability of the tissue was assessed by adding KCl (80 mM). Muscle contraction was observed by adding cumulative carbachol doses from 10^{-9} to 10^{-4} M. The relaxant effect of caftaric acid was measured against carbachol-induced contractions. This protocol was repeated by preincubating it with indomethacin (10 μM), propranolol (1 μM), 4DAMP (10 nM), atropine (10 μM), nifedipine (1 μM), glibenclamide (1 μM), barium chloride (4 mM), and methoctramine (1 μM) half an hour before carbachol administration to access the role of relevant receptors. The contractile force was analyzed by a LabChart 8 power lab data acquisition system (AD Instruments) connected to a computer.[34]

2.13. Statistical Analysis. The data were presented as mean ± SEM. The data obtained from various groups were statistically investigated by one-way and two-way analysis of variance (ANOVA) following Tukey's/Bonferroni's multiple comparison tests depending on the type of experiment by Graph Pad Prism version 8.0.2. $P < 0.05$ was considered as statistically significant.[10]

3. RESULTS

3.1. Effect of Caftaric Acid on the Expression of SOD, CAT, GSH, and iNOS. It has been evaluated that the expression of antioxidant enzymes (SOD, CAT, and GSH) reduced with a marked elevation of the oxidant enzyme (iNOS) level in the diseased significantly ($P < 0.05$) in comparison to that in control. Caftaric acid treatment (20, 40, and 60 mg/kg) restored these levels. Caftaric acid has shown a good response compared to mesna (Figure 1a).

3.2. Effect of Caftaric Acid on the Expression of Proinflammatory Cytokines IL-6, TGF 1-β, and TNF-α. The expression of pro-inflammatory cytokines IL-6, TGF 1-β, and TNF-α was significantly high in diseased relative to control. Caftaric acid treatment at all studied doses significantly ($P < 0.05$) decreased the proinflammatory cytokines relative to the diseased. Caftaric acid at these doses had shown more pronounced response then mesna (Figure 1b).

3.3. Effect of Caftaric Acid on Edema, Hemorrhage, Plasma Protein Extravasation, and Nociception. Edema, hemorrhage, and nociception were marked in diseased. An increased bladder wet weight was an indicator of edema, which was significantly ($P < 0.05$) high in diseased compared to that in control. Macroscopic examination showed hemorrhage in diseased (Table 1). Nociception measured as a decrease in locomotor activity together with behavioral changes had been profound in diseased. Plasma protein extravasation was significantly ($P < 0.05$) raised in diseased compared to control. Caftaric acid (20, 40, and 60 mg/kg) reversed the pathological characteristics of interstitial cystitis (Figure 2).

Table 1. Effect of Caftaric Acid on Edema and Hemorrhage

groups	edema	Hemorrhage
control	0	0
diseased (CYP 150 mg/kg)	3+	3+
mesna (40 mg/kg)	1+	0
caftaric acid (20 mg/kg)	2+	3+
caftaric acid (40 mg/kg)	1+	2+
caftaric acid (60 mg/kg)	0	1+

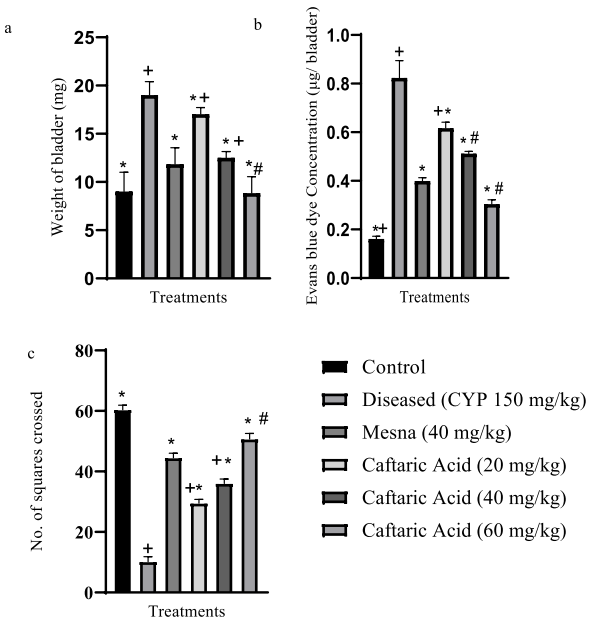

Figure 2. (a) Effect of caftaric acid on the weight of urinary bladder; (b) vascular permeability of Evans blue dye in urinary bladder; (c) number of squares crossed by rats in control, diseased (CYP, 150 mg/kg), mesna (40 mg/kg), and caftaric acid (20, 40 and 60 mg/kg). *$P < 0.05$, significant compared to diseased; $^{+}P < 0.05$, significant compared to mesna; and $^{\#}P < 0.05$, nonsignificant compared to mesna. One-way ANOVA, followed by Tukey's multiple comparison test; $n = 6$. Vertical bars represent SEM.

3.4. DPPH Radical Scavenging Effect of Caftaric Acid. The radical scavenging activity was presented as the quantity of antioxidant required to decline the initial absorbance of DPPH by 50% (IC_{50}). Graphical method was used to determine the IC_{50} values of both ascorbic acid and caftaric acid. The graph was built as a percentage disappearance of DPPH against each sample concentration. IC_{50} of caftaric acid was 5.455 ± 11 mg/mL as compared with ascorbic acid (5.682 ± 11 mg/mL).

3.5. Effect of Caftaric Acid on Histopathology. Bladder tissues had been analyzed for the pathological changes. Edema, hemorrhage, urothelium destruction, and lymphocyte infiltration were determined by H&E staining, while Periodic acid Schiff staining determined glycosaminoglycan integrity. Control shows normal bladder with no edema, hemorrhage,

https://doi.org/10.1021/acsomega.3c01450
ACS Omega 2023, 8, 28196−28206

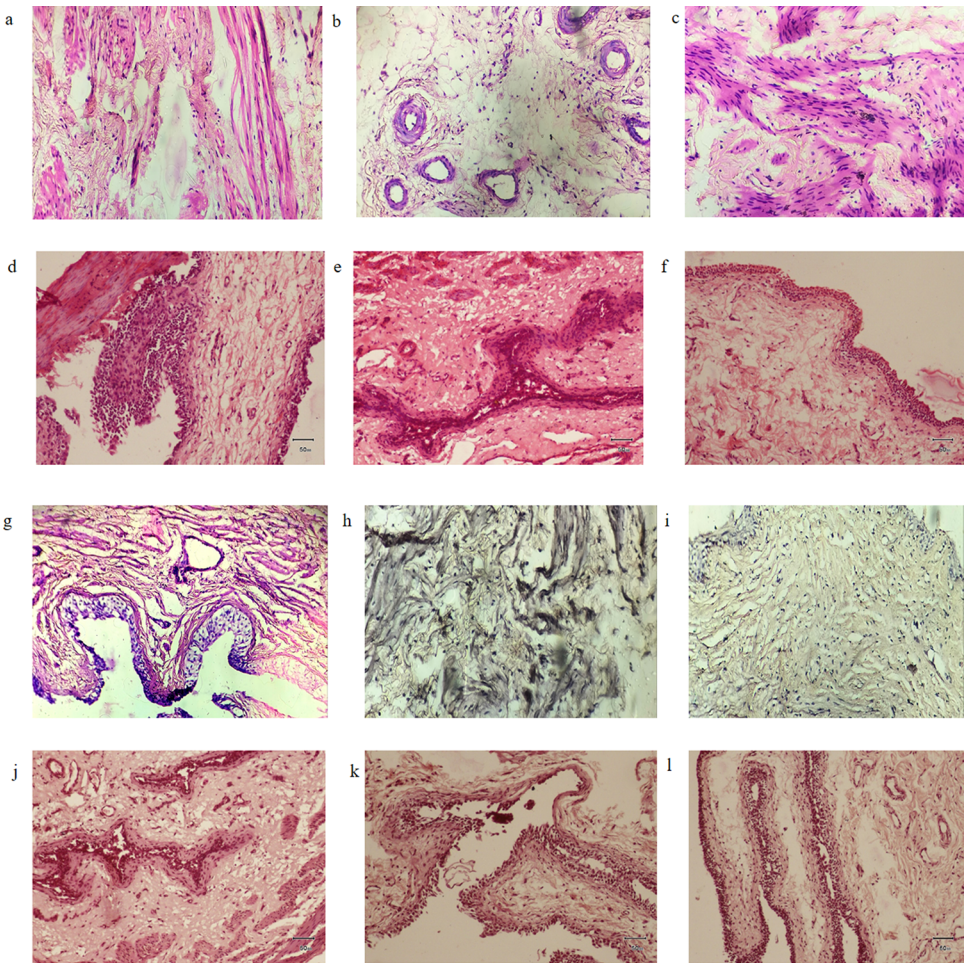

Figure 3. Histological examination of Control, cyclophosphamide (CYP)-treated, and caftaric acid-treated female rat bladders. Bladders fixed in 10% formalin, cryopreserved, cut serially into 20 μm sections, and stained with hematoxylin−eosin (H&E). Original magnification, ×10. (a) Control showing normal bladder; (b) cyclophosphamide (CYP 150 mg/kg)-treated showing sloughing and degeneration of transitional epithelium and marked edema with inflammatory infiltrate; (c) mesna-treated (40 mg/kg) showing almost normal tissue; (d) caftaric acid (20 mg/kg) to CYP post-treated rats showing marked proliferation of epithelial cells and hemorrhage; (e) caftaric acid (40 mg/kg) to CYP post-treated rats showing sloughing and denudation of epithelium; (f) caftaric acid (60 mg/kg) to CYP post-treated rats showing almost normal epithelium with no denudation. Periodic acid-Schiff (PAS) staining of (g) control showing normal bladder urothelium with intact GAG layer, (h) diseased (CYP-treated, 150 mg/kg) showing damaged transitional epithelium and GAG layer; (i) mesna-treated (40 mg/kg) showing regular GAG layer, (j) caftaric acid (20 mg/kg) to CYP post-treated rats showing markedly damaged GAG layer; (k) caftaric acid (40 mg/kg) to CYP post-treated rats showing least damaged GAG layer; and (l) caftaric acid (60 mg/kg) to CYP post-treated rats showing almost normal intact GAG layer.

Table 2. Interaction of Caftaric Acid and Mesna with Various Antioxidant and Proinflammatory Cytokine Receptors

receptor	active compound	PDB ID	binding energy (kcal/mol)	inhibition constant (ki) (nM)	torsional energy	no. of hydrogen bonds	interacting residues
catalase-caf	CAT	1DGB	−7.14	5.86	2.09	1	LEU721, GLU723, LEU726, TRP755, MET759, LEU763, PHE778, LEU797, LEU887, TYR890,
glutathione-caf	GSH	3DK4	−10.92	9.87	2.09	3	PRO160, SER161, THR176, SER177, GLY196, TYR197, ILE198, TRP287, ALA288, ILE289, GLY290
cytokine-caf	IL-6	4ZS7	−8.5	583.45	2.09	2	GLN3, LEU4, GLY27, TRP36, ARG99, TYR111, TYR112, GLY113, GLN114
tumor necrosis factor-caf	TNF-α	4TWT	−10.15	36.52	2.09	4	ALA96, LYS98, PRO117, ILE118, TYR119
catalase-mes	CAT	1DGB	−4.51	496.9	0.3	1	LEU26, PRO78, THR79, LEU80, VAL132, LEU134
glutathione-mes	GSH	3DK4	−5.01	210.95	0.3	2	GLY29, SER30, GLY56, THR57, CYS58, THR339
cytokine-mes	IL-6	4ZS7	−4.87	270.44	0.3	1	LEU47, GLU48, TRP49, ARG94, ALA99, VAL100, PHE101S
tumor necrosis factor-mes	TNF-α	4TWT	−4.67	379.61	0.3	2	VAL17, PHE144, GLU146, GLY148, GLN149, VAL150, TYR151

https://doi.org/10.1021/acsomega.3c01450
ACS Omega 2023, 8, 28196−28206

urothelial damage, and lymphocyte infiltration (Figure 3a), while the diseased cyclophosphamide (CYP)-treated (150 mg/kg) samples show sloughing and degeneration of transitional epithelium and marked edema with inflammatory infiltrate (Figure 3b); mesna pretreatment (40 mg/kg) showed almost normal intact tissue (Figure 3c), and caftaric acid (20, 40, and 60 mg/kg) to CYP post-treated rats restored bladder tissue architecture (Figure 3d−f). Periodic acid-Schiff (PAS) staining of the control shows normal bladder urothelium with an intact GAG layer (Figure 3g), while the diseased showed damaged transitional epithelium and GAG layer (Figure 3h); mesna-treated sample (40 mg/kg) shows a regular GAG layer (Figure 3i), and caftaric acid (20, 40, and 60 mg/kg) to CYP post-treated rats restored the urothelium and the GAG layer (Figure 3j−l).

3.6. Docking Studies. The three-dimensional coordinates of caftaric acid and mesna had been retrieved from PubChem with their respective PubChem CIDs. The affinity of caftaric acid and mesna with antioxidant enzymes (CAT and GSH) and proinflammatory cytokines (IL-6 and TNF-α) are tabulated in Table 2. It is clear from Table 2 that caftaric acid represents the best interaction at the GSH receptor (3DK4) for antioxidant activity, along with the least binding energy of −10.92 kcal/mol. The main interacting residues of caf at the 3DK4 receptor are PRO160, SER161, THR176, SER177, GLY196, TYR197, ILE198, TRP287, ALA288, ILE289, and GLY290 (Figure 4c) with three hydrogen and one hydrophobic interactions shown in Figure 4a,b. On the other hand, caftaric acid also shows the best anticancer activity at the TNF-α (4TWT) receptor, presenting the least binding energy of −10.15 kcal/mol. As it is clear from Figure 4d, the main interacting residues of 4TWT with caftaric acid include ALA96, LYS98, PRO117, ILE118, and TYR119, along with three hydrophobic and three hydrogen bonds. Caftaric acid also represents π-stacking and salt bridge, as shown in Figure 4e,f. In comparison, mesna presents poor interaction at the GSH receptor (3DK4) with the least binding energy of −5.01 kcal/mol and two hydrogen bonds. The main interacting amino acid residues of mesna at the 3DK4 receptor are GLY29, SER30, GLY56, THR57, CYS58, and THR339, as shown in Figure 4h. The hydrogen-bond interaction of mesna at the 3KD4 receptor is shown in Figure 4g. In addition to previous results, mesna also represents poor interactions at the TNF-α (4TWT) receptor. The least binding energy of mesna at the 4TWT receptor was found to be −4.67 kcal/mol along with the interacting amino acid residues including VAL17, PHE144, GLU146, GLY148, GLN149, VAL150, and TYR151, as evident from Figure 4j. Three hydrogen bonds formed by mesna at the 4TWT receptor are shown in Figure 4i.

3.7. Effect of Caftaric Acid on Isolated Rat Bladder Strips. *3.7.1. Carbachol-Induced Contraction in Isolated Bladder Strips.* Contractions to carbachol have been expressed as the percentage of contraction response to 80 mM K^+. The carbachol-induced contractions were increased (213.25 ± 0.85) significantly in CYP-treated animals compared to control (Figure 5a).

3.7.2. Relaxant Effect of Caftaric Acid Against Carbachol-Induced Contraction in Isolated Bladder Strips. The cumulative caftaric acid (10^{-8} to 10^{-5} M) relaxation response against carbachol-induced contraction was significant in both control and diseased (Figure 5b). The EC_{50} values of control ($8.432 \times 10^{-9} \pm 5$ M) were significantly ($P < 0.05$) higher than that of CYP-treated samples ($1.590 \times 10^{-8} \pm 5$ M).

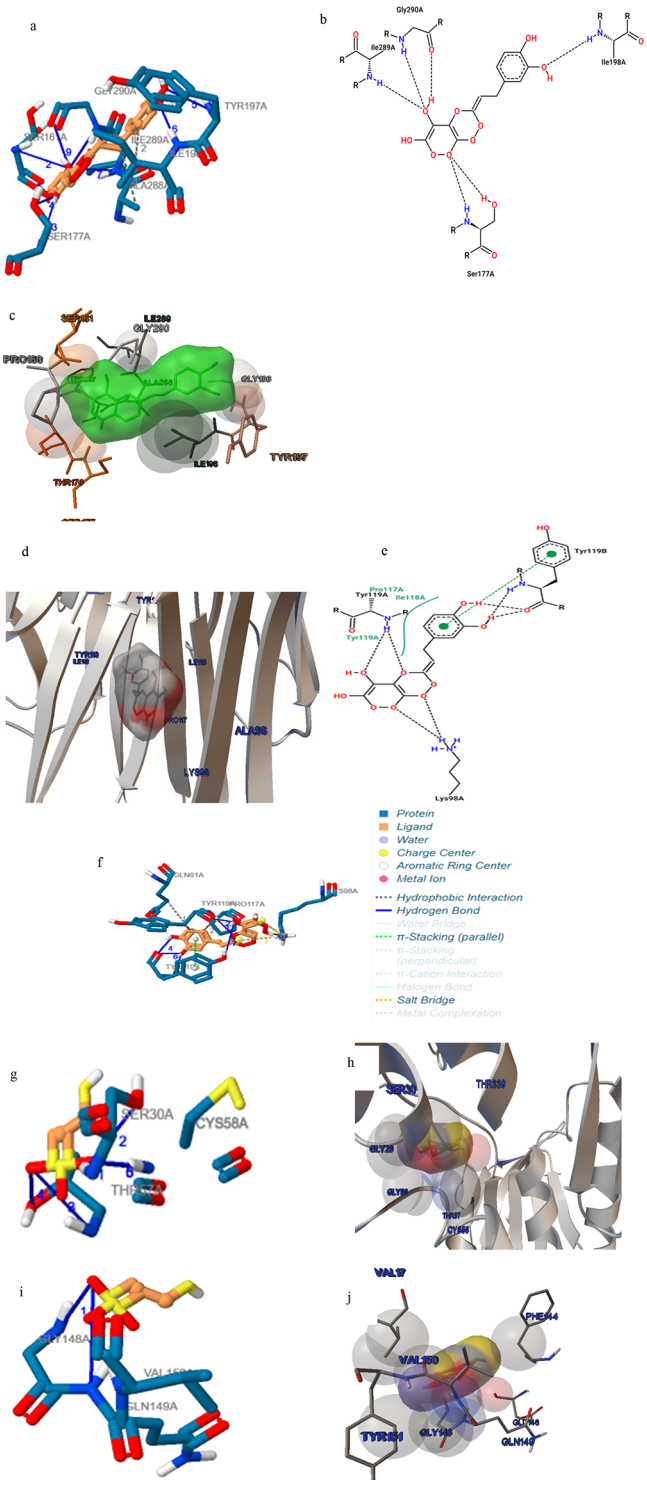

Figure 4. (a) Ligand (caftaric acid) shown as a yellow stick, with the interacting amino acid residues (blue sticks) showing hydrogen bonding as a blue straight line and hydrophobic interaction as a gray dotted line. (b) Interacting amino acids forming hydrogen bonds in the binding pocket of 3KD4 receptor obtained from the protein plus online software. (c) Best docked structure of the ligand (green colored/caftaric acid) in coordination with the amino acid residues of 3DK4 (GSH) enzyme with the binding energy of −10.92 (kcal/mol). (d) Caftaric acid (in gray-red sphere) present inside the binding pocket of 4TWT (TNF-α), with amino acid residues of the best docked pose having a binding energy of −10.15 kcal/mol, calculated from Auto Dock Tools 1.5.6 software. (e) Interacting amino acids forming hydrogen bonds (black dotted line) and π-stacking of

https://doi.org/10.1021/acsomega.3c01450
ACS Omega 2023, 8, 28196−28206

Figure 4. continued

aromatic rings (green dotted line), obtained from protein plus software. (f) Yellow-colored ligand (caftaric acid) interacting with blue-colored amino acid residues forming hydrogen bonds (blue straight line) and hydrophobic interactions (as gray dotted line) along with π-stacking (shown as green dotted line) and salt-bridge formation (yellow dotted line) obtained from PLIP online software. (g) Ligand (mesna) shown as a yellow stick interacting with blue-colored amino acid residues, showing hydrogen bonding as a blue straight line. (h) Mesna (inside red-yellow sphere) in the binding pocket of 3DK4 (GSH; shown as a secondary structure) with the surrounding amino acid residues with a binding energy of −5.01 (kcal/mol) obtained from Auto Dock Tools 1.5.6 software. (i) Interacting amino acid residues shown as a blue stick in the binding pocket of 4TWT, forming hydrogen bonds (blue straight line) with mesna shown as a yellow stick. (j) Ligand (mesna/red-yellow sphere) interaction with amino acid residues (shown as sticks) in the binding pockets of 4TWT (TNF-α) with the binding energy, −4.67 (kcal/mol).

3.7.3. Role of Muscarinic Receptors on the Relaxant Effect of Caftaric Acid. In order to find the involvement of muscarinic receptors, a nonselective muscarinic receptor blocker atropine (10 μM), M3-selective blocker 4DAMP (10 nM), and M2-selective blocker methoctramine (1 μM) have been used. Both atropine and 4DAMP completely abolished the relaxation response of caftaric acid in both control and diseased (Figure 5c−f), while preincubation with methoctramine produces equal responses in both the control and diseased strips to caftaric acid (Figure 5g,h). The EC_{50} values of methoctramine-preincubated control strips ($4.017 \times 10^{-8} \pm 5$ M) were similar to that of diseased ($4.439 \times 10^{-8} \pm 5 \pm 1$ M).

3.7.4. Role of Calcium Channels on the Relaxant Effect of Caftaric Acid. The calcium channel blocker nifedipine (1 μM) decreased caftaric acid relaxation significantly ($P < 0.5$) to 10 ± 0.4% and 16 ± 0.6% in control and diseased rats (Figure 5c,d). The EC_{50} values of nifedipine-preincubated control strips ($3.581 \times 10^{-6} \pm 5$ M) were slightly high than that of diseased ($3.035 \times 10^{-6} \pm 5$ M).

3.7.5. Role of ATP-Sensitive Potassium Channel on the Relaxant Effect of Caftaric Acid. Glibenclamide (1 μM), an ATP-sensitive potassium channel blocker, lessened the relaxation effect of caftaric acid significantly ($P < 0.5$) to 53 ± 2.2% in control and 73 ± 0.8% in diseased (Figure 5c,d). The EC_{50} value for glibenclamide-preincubated strips was high in diseased ($7.642 \times 10^{-8} \pm 5$ M) relative to that of the control ($4.109 \times 10^{-8} \pm 5$ M).

3.7.6. Role of Inward Rectified Potassium Channel on the Relaxant Effect of Caftaric Acid. Barium chloride (4 mM), an inward rectified potassium channel blocker, did not decrease the relaxation response of caftaric acid in both control and diseased. It showed a nonsignificant response to control and diseased ($P < 0.5$) groups (Figure 5g,h). In the diseased group, the EC_{50} value of barium chloride-preincubated strips was ($2.943 \times 10^{-8} \pm 5$ M), more in comparison to that of control ($1.604 \times 10^{-8} \pm 5$).

3.7.7. Role of β- Adrenergic Receptors on the Relaxant Effect of Caftaric Acid. A nonselective β-adrenergic receptor blocker propranolol (1 μM) nonsignificantly ($P < 0.5$) reduces the relaxation produced by caftaric acid in control (86 ± 1.4%) while decreasing significantly ($P < 0.5$) in diseased (75 ± 1.2%) (Figure 5e,f). In propranolol-preincubated strips, EC_{50} was low in diseased ($6.123 \times 10^{-8} \pm 5$ M) comparative to that in control ($1.409 \times 10^{-7} \pm 5$ M).

3.7.8. Role of Cyclooxygenase Enzyme on the Relaxant Effect of Caftaric Acid. Indomethacin (10 μM) inhibits prostaglandin synthesis via blocking the cyclooxygenase enzyme. In controlled rat bladder strips, it decreases the relaxant effect with caftaric acid significantly ($P < 0.5$) to 45.8 ± 2.2%, while in diseased to 76 ± 1.2% (Figure 5e,f). EC_{50} was higher in the diseased group ($2.681 \times 10^{-8} \pm 5$ M) relative to the control ($1.550 \times 10^{-8} \pm 5$ M) group.

4. DISCUSSION

Cyclophosphamide (CYP) is a chemotherapeutic agent used in the treatment of tumors and autoimmune disorders. The high dose of CYP damages liver, kidney, and urinary bladder. One-fourth of patients taking this medicine complained of severe interstitial cystitis (IC).[35] Its metabolite acrolein is produced in the liver. It is acrolein that produces the pathological features of IC upon accumulating in the bladder. Mesna is used as a preventive drug. It generates a sulfhydryl group while interacting with glutathione reductase that neutralizes acrolein, promoting its excretion. Mesna, however, does not completely resolve the pathological features, as subclinical IC exists even after use. It is also not safe as the patient undergoing preventive mesna therapy complaints severe systemic adverse effects and cutaneous hypersensitivity reactions. This offers space for the search of safe alternative pharmacological agents.[36] Caftaric acid is a phenol which showed antioxidant and gastroprotective activity.[17] This study aimed to find the uroprotective potential of caftaric acid. Hence, its anti-inflammatory, antioxidant, and smooth muscle relaxant effects with mechanisms were investigated.

Urothelium ulceration, hemorrhage, edema, infiltration of inflammatory cells, and nociception are the main pathological features of IC. Acrolein is the main culprit for the development of these features. It upregulates the production of ROS and NO through many pathways, leading to oxidative stress and inflammation.[6] Our study demonstrates that caftaric acid has antioxidant, anti-inflammatory, and smooth muscle relaxant properties.

In order to find the antioxidant potential of caftaric acid, we measured the oxidant stress markers of the cells, SOD, CAT, GSH, and iNOS, and to determine the anti-inflammatory potential, we measured the expression of proinflammatory cytokines, IL-6, TGF 1-β, and TNF-α. ROS alters the natural defense in the bladder, which is evident from the decreased expression of antioxidants SOD, CAT, and GSH. These are important components of a cell's natural defense against oxidants. The expression of iNOS is however raised, associated with the increased NO production. The previous findings are consistent with our study results.[37] Molecular oxygen generates several reactive intermediates that destroy cellular structures and functions upon CYP injection. Antioxidants like luteolin and boswellic acid showed protective response against IC in previous studies. Current study shows that caftaric acid pretreatment improves the bladder expression of oxidant defense (SOD, CAT, and GSH) while decreasing the inflammatory enzyme (iNOS) and cytokine expression (IL-6, TGF 1-β, and TNF-α) in a dose-dependent manner compared to the diseased. Caftaric acid shows better response compared to mesna-treated. The antioxidant capacity of caftaric acid was further demonstrated through the DPPH assay. DPPH has an odd electron that gives deep purple color and absorbance at

https://doi.org/10.1021/acsomega.3c01450
ACS Omega 2023, 8, 28196−28206

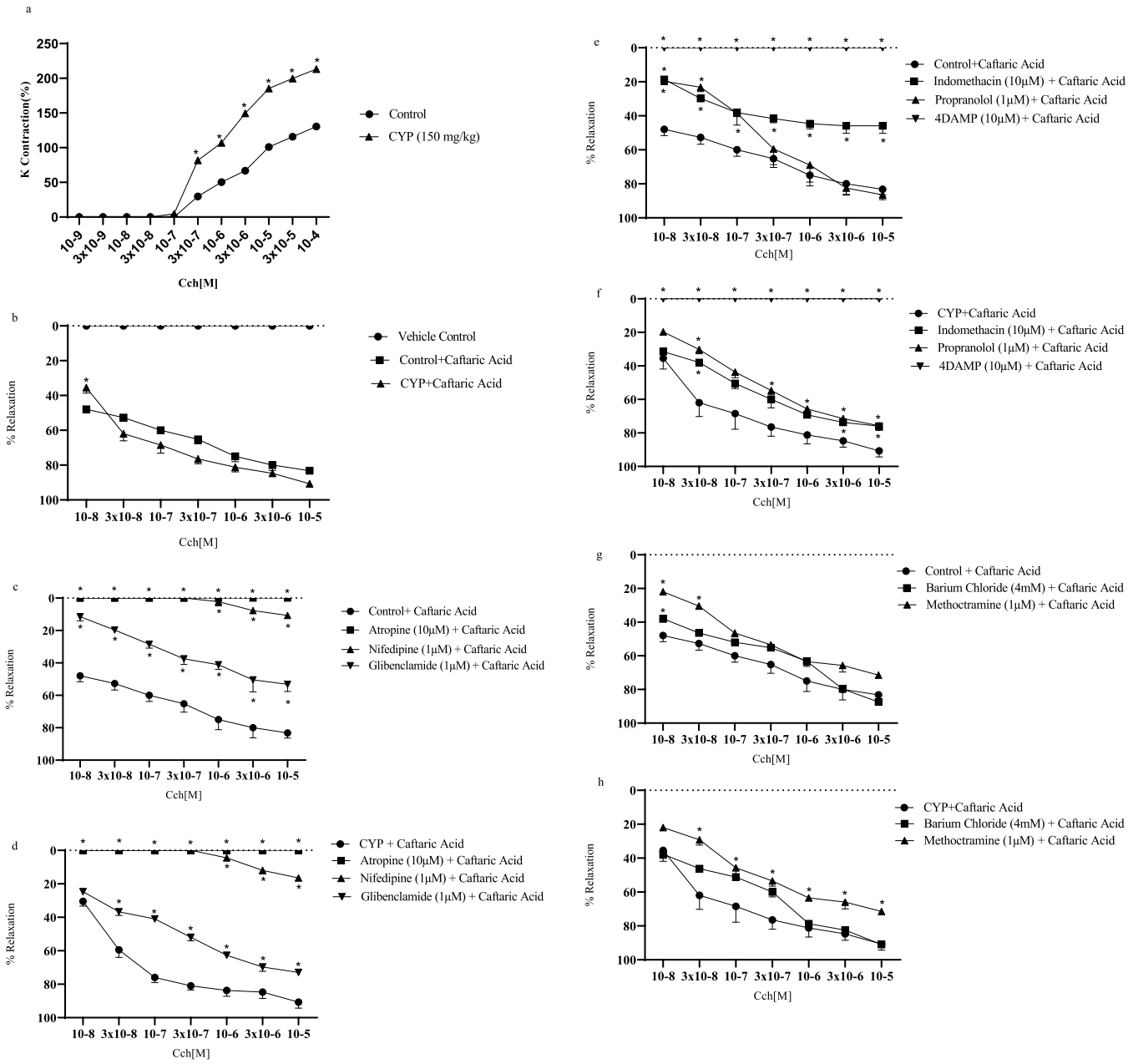

Figure 5. (a) Cumulative carbachol (Cch) response curves (10^{-9} to 10^{-4}) in isolated rat bladder strips from control and cyclophosphamide-treated rats. (b) Cumulative caftaric acid response curves (10^{-8} to 10^{-5}) in isolated rat bladder strips from control, vehicle control, and cyclophosphamide-treated rats. (c) Cumulative caftaric acid response curves (10^{-8} to 10^{-5}) in isolated rat bladder strips alone and in the presence of atropine (10 μM), nifedipine (1 μM), and glibenclamide (1 μM). (d) Cumulative caftaric acid response curves (10^{-8} to 10^{-5}) in cyclophosphamide-treated isolated rat bladder strips alone and in the presence of atropine (10 μM), nifedipine (1 μM), and glibenclamide (1 μM). (e) Cumulative caftaric acid response curves (10^{-8} to 10^{-5}) in isolated rat bladder strips alone and in the presence of indomethacin (10 μM), propranolol (1 μM), and 4DAMP (10 nM). (f) Cumulative caftaric acid response curves (10^{-8} to 10^{-5}) in cyclophosphamide-treated isolated rat bladder strips alone and in the presence of indomethacin (10 μM), propranolol (1 μM), and 4 DAMP (10 nM). (g) Cumulative caftaric acid response curves (10^{-8} to 10^{-5}) in isolated rat bladder strips alone and in the presence of barium chloride (4 mM) and methoctramine (1 μM). (h) Cumulative caftaric acid response curves (10^{-8} to 10^{-5}) in cyclophosphamide-treated isolated rat bladder strips alone and in the presence of barium chloride (4 nM) and methoctramine (1 μM). Data have been presented as mean ± SEM. *$P < 0.05$, significant compared to that treated with caftaric acid alone; $n = 6$. Two-way ANOVA, followed by Bonferroni's/Tukey's multiple comparison test.

517 nm. Compounds with antioxidant property donate an electron to DPPH which is visible through a change in color and decrease in absorbance. Caftaric acid possesses an antioxidant activity equivalent to ascorbic acid. Plant polyphenols possess radicals that delocalize and stabilize unpaired electrons.[25] Thus, caftaric acid has antioxidant and anti-inflammatory activities.[6,20,33]

Molecular docking is an important in silico method utilized in the discovery of drugs to virtually screen many compounds in virtual libraries comprising millions of molecular structures with diverse drug targets of known three-dimensional structures. Molecular modeling method provides insights into the ligand's binding affinity with the target's active binding site, adopting a variety of binding modes.[38] In silico computational

https://doi.org/10.1021/acsomega.3c01450
ACS Omega 2023, 8, 28196−28206

studies were utilized to show the antioxidant property of phytochemicals against three enzymes: SOD, CAT, and GSH.[39] Our study showed that caftaric acid has good interaction with antioxidants (CAT and GSH) and anticancer enzymes (TNF-α and IL6) compared to mesna. The docking score of the best antioxidant receptor 3DK4 with caftaric acid was −10.92 kcal/mol, in comparison to mesna, representing a binding energy of −5.01 kcal/mol. While comparing the anticancer potentials, mesna presents the least binding energy of −4.67 kcal/mol at the 4TWT receptor; again, caftaric acid represents a greater binding affinity at the same receptor with the binding energy of −10.15 kcal/mol, thus showing more potential for anticancer receptors. It inhibits oxidant enzymes and proinflammatory cytokines. It was reported that compounds that show an inhibitory potential with iNOS, TNF-α, IL-6, and TGF 1-β had good anti-inflammatory potential.[40−42]

Acrolein accumulation in bladder destroys the structural architecture through phenoxynitrite and ROS production.[43] It has been determined that caftaric acid plays a role in resolving edema, hemorrhage, and nociception. Increase in bladder weight reflects edema. Increase in protein extravasation, hemorrhage, and vasodilation depicts inflammation. In the present study, histopathological analysis shows sloughing and destruction of transitional epithelium with large inflammatory infiltrates, GAG destruction, and edema in diseased. Bladder wet weight is also increased in diseased. Caftaric acid at all studied doses gradually improves bladder architecture, as reflected by decreasing edema and hemorrhage score, bladder wet weight, Evans blue dye extravasation, and increasing locomotor activity index. It was reported earlier that the migration of macrophages occurred in urinary bladder. These cells produce proinflammatory cytokines (IL-6, TGF 1-β, and TNF-α). TNF-α and IL-6 produce hyperalgesia in rats.[44] TNF-α is further responsible for iNOS induction that exerts cytotoxic effect directly through phenoxynitrite production or indirectly. It destroys urothelium, GAG layer, and capillary leakage and produces edema.[9] TGF 1-β is an important cytokine that causes pathological changes in the bladder epithelium and detrusor mastocytosis.[5] Hence, the protective response of caftaric acid in CYP-induced IC by downregulating inflammatory cytokines is observed.

A set of experiments were performed on isolated rat bladder strips from control and diseased rats. The strips were preincubated with various receptors, channels, and enzyme blockers to determine the possible mechanisms involved in the relaxant response of caftaric acid. To determine the possible involvement of muscarinic receptors, ATP-sensitive potassium channel opening, inward rectified potassium channel, calcium channels, ß-adrenergic receptors, and cyclooxygenase enzyme in the relaxation of the bladder smooth muscles, the strips were preincubated with methoctramine (1 μM), atropine (10 μM), 4 DAMP (10 nM), glibenclamide (1 μM), barium chloride (4 mM), nifedipine (1 μM), propranolol (1 μM), and indomethacin (10 μM) in both control and CYP-treated rats, respectively.

All subtypes of muscarinic receptors (M_1−M_5) were found in bladder. Muscarinic M_2 and M_3 were found in the urothelium and detrusor smooth muscles. The major contractile response upon cholinergic stimulation is due to M_3 receptors. Its expression is however changed in diseases like IC.[45] The contractile response of carbachol (M_3 agonist) was increased significantly in diseased in comparison to that in control, while the contraction observed with 80 mM K remained the same in both.[7] Caftaric acid had relaxation response in both the control and diseased rat strips. A higher relaxation response was observed in diseased compared to that in control.

Administration of atropine (10 μM) and 4 DAMP (10 nM) inhibited carbachol-induced contractile response equally in both the control and diseased strips. The results indicate that caftaric acid produces smooth muscle relaxation by inhibiting M_3 receptors. Methoctramine (1 μM) shows equal and nonsignificant response compared to caftaric acid in both control and diseased, suggesting the noninvolvement of M_2receptor blockade in caftaric acid relaxant response.[45] To determine the involvement of ATP-sensitive potassium channel, its blocker glibenclamide (1 μM) was added to both. In diseased, more relaxation was observed compared to control, indicating its role in caftaric acid relaxation. However, inward-rectified potassium channels were observed to have no participation in the relaxation of caftaric acid. Nonsignificant equal response is observed in both diseased and control when barium chloride (4 mM) was administered.[46]

The relaxation was decreased significantly in diseased and control strips when preincubated with nifedipine (1 μM), pointing to calcium channel blocking as one of the mechanisms involved in relaxation.[47] The role of beta-adrenergic receptors was determined by adding propranolol (1 μM). It does not decrease the relaxation in control but decreases slightly in the diseased. The involvement of COX enzyme was evaluated by giving indomethacin (10 μM). The relaxant effect was decreased more significantly in control compared to diseased. It could be one of the possible mechanisms of relaxation as reported previously.[48,49]

5. CONCLUSIONS

The present study suggested that caftaric acid has antioxidant, anti-inflammatory, and bladder smooth muscle relaxation activities which were the main concerns in the pathophysiology of IC. It has antioxidant potential comparable to ascorbic acid. It increases SOD, CAT, and GSH while decreases iNOS, IL-6, TGF 1-β, and TNF-α. In silico studies further confirmed the antagonizing potential of various antioxidant and proinflammatory cytokine receptors (CAT, GSH, TNF-α, and IL-6) with caftaric acid in comparison to mesna. It restores normal bladder tissue, decreases edema, hemorrhage, Evans blue dye extravasation, and nociception. It shows bladder muscle relaxation against carbachol-induced contraction involving the possible blockade of M_3 receptor, ATP-sensitive potassium channels, calcium channels, and prostaglandin synthesis inhibition. However, M_2 receptors, inward-rectified potassium channels, and beta-adrenergic receptor were not involved in relaxation. These findings propose that caftaric acid could be used as a therapeutic alternative in the treatment of cyclophosphamide-induced interstitial cystitis.

AUTHOR INFORMATION

Corresponding Author

Irfan Anjum − *Faculty of Pharmacy, The University of Lahore, Lahore 55150, Pakistan;* Present Address: Department of Basic Medical Sciences, Shifa College of Pharmaceutical Sciences, Shifa Tameer-e-Millat University, Islamabad, 44000, Pakistan; orcid.org/0000-0001-5884-8950; Email: anjuum95@yahoo.com

https://doi.org/10.1021/acsomega.3c01450
ACS Omega 2023, 8, 28196−28206

Authors

Saima − *Faculty of Pharmacy, The University of Lahore, Lahore 55150, Pakistan*

Saima Najm − *Department of Pharmacy, Lahore College of Pharmaceutical Sciences, Lahore 55150, Pakistan;* orcid.org/0000-0002-2588-7037

Kashif Barkat − *Faculty of Pharmacy, The University of Lahore, Lahore 55150, Pakistan*

Hiba-Allah Nafidi − *Department of Food Science, Faculty of Agricultural and Food Sciences, Laval University, Quebec City, Quebec G1V 0A6, Canada*

Yousef A. Bin Jardan − *Department of Pharmaceutics, College of Pharmacy, King Saud University, Riyadh 11451, Saudi Arabia*

Mohammed Bourhia − *Laboratory of Chemistry and Biochemistry, Faculty of Medicine and Pharmacy, Ibn Zohr University, Laayoune 70000, Morocco;* orcid.org/0000-0003-3707-8461

Complete contact information is available at: https://pubs.acs.org/10.1021/acsomega.3c01450

Author Contributions

Saima: data collection and writing manuscript. I.A., H.N., Y.B.J., M.B.: conceptualization, methodology, interpretation, review, and editing. S.N.: molecular docking. K.B.: results interpretation. All authors have read and agreed to the submitted version.

Funding

This work was financially supported by the Researchers Supporting Project (RSP2023R457), King Saud University, Riyadh, Saudi Arabia.

Notes

The authors declare no competing financial interest.

■ ACKNOWLEDGMENTS

The authors would like to extend their sincere appreciation to the Researchers Supporting Project, King Saud University, Riyadh, Saudi Arabia, for funding this work through the project number (RSP2023R457). The authors thank the lab staff of Powerlab, Faculty of Pharmacy, The University of Lahore, Lahore, and University of Health Sciences, Lahore, Pakistan.

■ ABBREVIATIONS

4 DAMP, 4-diphenylacetoxy-*N*-methylpiperidine; ANOVA, analysis of variance; AP-1, activator protein-1; $C_6H_{12}O_6.H_2O$, glucose monohydrate; $CaCl_2$, calcium chloride; CAT, catalase; cDNA, complementary deoxyribonucleic acid; CMC Na, carboxymethylcellulose sodium; DMF, dimethylformamide; DMSO, dimethyl sulfoxide; DPPH, 1,1-diphenyl-picrylhydrazyl; GAG, glycosamine glycan; H&E, hematoxylin−eosin; HRPT, hypoxanthine−guanine phosphoribosyltransferase; IC, interstitial cystitis; IL-6, interleukin-6; iNOS, inducible nitric oxide synthase; IP, intraperitoneal route; KCl, potassium chloride; KH_2PO_4, potassium dihydrogen phosphate; LGA, Lamarckian genetic algorithm; $MgSO_4$, magnesium sulfate; NaCl, sodium chloride; $NaHCO_3$, sodium bicarbonate; NF-κB, nuclear factor-κB; PAS, periodic acid-Schiff; PDB, Protein Data Bank; qPCR, quantitative polymerase chain reaction; RMSD, root-mean-square deviation; RSC, free-radical scavenging capacity; SEM, standard error of mean; SOD, superoxide dismutase; TGF 1-β, transforming growth factor 1-β; TNF-α, tissue necrosis factor-α; TRI, trizol

■ REFERENCES

(1) He, Y. Q.; Zhang, W. T.; Shi, C. H.; Wang, F. M.; Tian, X. J.; Ma, L. L. Phloroglucinol protects the urinary bladder via inhibition of oxidative stress and inflammation in a rat model of cyclophosphamide-induced interstitial cystitis. *Chin. Med. J.* **2015**, *128*, 956−962.

(2) Chung, J. W.; Chun, S. Y.; Lee, E. H.; Ha, Y. S.; Lee, J. N.; Song, P. H.; Yoo, E. S.; Kwon, T. G.; Chung, S. K.; Kim, B. S. Verification of mesenchymal stem cell injection therapy for interstitial cystitis in a rat model. *PLoS One* **2019**, *14*, No. e0226390.

(3) Büyüknacar, H. S.; Kumcu, E. K.; Göçmen, C.; Önder, S. Effect of phosphodiesterase type 4 inhibitor rolipram on cyclophosphamide-induced cystitis in rats. *Eur. J. Pharmacol.* **2008**, *586*, 293−299.

(4) Wróbel, A.; Serefko, A.; Bańczerowska-Górska, M.; Szopa, A.; Dudka, J.; Poleszak, E. Intravesical administration of blebbistatin prevents cyclophosphamide-induced toxicity of the urinary bladder in female Wistar rats. *Neurourol. Urodyn.* **2019**, *38*, 1044−1052.

(5) Gonzalez, E. J.; Girard, B. M.; Vizzard, M. A. Expression and function of transforming growth factor-β isoforms and cognate receptors in the rat urinary bladder following cyclophosphamide-induced cystitis. *Am. J. Physiol.* **2013**, *305*, F1265−F1276.

(6) Fatima, M.; Anjum, I.; Abdullah, A.; Abid, S. Z.; Malik, M. N. H. Boswellic Acids, Pentacyclic Triterpenes, Attenuate Oxidative Stress, and Bladder Tissue Damage in Cyclophosphamide-Induced Cystitis. *ACS Omega* **2022**, *7*, 13697−13703.

(7) Anjum, I.; Denizalti, M.; Kandilci, H. B.; Durlu-Kandilci, N. T.; Sahin-Erdemli, I. Enhancement of S1P-induced contractile response in detrusor smooth muscle of rats having cystitis. *Eur. J. Pharmacol.* **2017**, *814*, 343−351.

(8) Nasrin, S.; Masuda, E.; Kugaya, H.; Ito, Y.; Yamada, S. Improvement by phytotherapeutic agent of detrusor overactivity, down-regulation of pharmacological receptors and urinary cytokines in rats with cyclophosphamide induced cystitis. *J. Urol.* **2013**, *189*, 1123−1129.

(9) Korkmaz, A.; Topal, T.; Oter, S. Pathophysiological aspects of cyclophosphamide and ifosfamide induced hemorrhagic cystitis; implication of reactive oxygen and nitrogen species as well as PARP activation. *Cell Biol. Toxicol.* **2007**, *23*, 303−312.

(10) Andersson, M.; Aronsson, P.; Doufish, D.; Lampert, A.; Tobin, G. Muscarinic receptor subtypes involved in urothelium-derived relaxatory effects in the inflamed rat urinary bladder. *Auton. Neurosci.* **2012**, *170*, 5−11.

(11) Wróbel, A.; Zapała, Ł.; Kluz, T.; Rogowski, A.; Misiek, M.; Juszczak, K.; et al. The potential of asiatic acid in the reversion of cyclophosphamide-induced hemorrhagic cystitis in rats. *Int. J. Mol. Sci.* **2021**, *22*, 5853.

(12) Ribeiro, R. A.; Lima-Junior, R. C.; Leite, C. A. V. G.; Mota, J. M. S. C.; Macedo, F. Y.; Lima, M. V.; Brito, G. A. Chemotherapy-induced hemorrhagic cystitis: pathogenesis, pharmacological approaches and new insights. *J. Exp. Integr. Med.* **2012**, *2*, 95−112.

(13) Yildiz, S. C.; Keskin, C.; Sahinturk, V.; Ayhanci, A. Investigation of uroprotective effects of seed methanol extracts of Hypericum triquetrifolium Turra. on cyclophosphamide-induced bladder hemorrhagic cystitis and nephrotoxicity in Wistar albino rats. *Çukurova Med. J.* **2020**, *45*, 1361−1371.

(14) Gonçalves, R. L. G.; Cunha, F. V. M.; Sousa-Neto, B. P. S.; Oliveira, L. S. A.; Lopes, M. E.; Rezende, D. C.; Oliveira, F. D. A. α-Phellandrene attenuates tissular damage, oxidative stress, and TNF-α levels on acute model ifosfamide-induced hemorrhagic cystitis in mice. *Naunyn-Schmiedeb. Arch. Pharmacol.* **2020**, *393*, 1835−1848.

(15) Cheynier, V. F.; Van Hulst, M. W. Oxidation of trans-caftaric acid and 2-S-glutathionylcaftaric acid in model solutions. *J. Agric. Food Chem.* **1988**, *36*, 10−15.

(16) Gonthier, M. P.; Remesy, C.; Scalbert, A.; Cheynier, V.; Souquet, J. M.; Poutanen, K.; Aura, A. M. Microbial metabolism of caffeic acid and its esters chlorogenic and caftaric acids by human faecal microbiota in vitro. *Biomed. Pharmacother.* **2006**, *60*, 536−540.

(17) Tanyeli, A.; Akdemir, F.; Eraslan, E.; Güler, M.; Nacar, T. Anti-oxidant and anti-inflamatuar effectiveness of caftaric acid on gastric

ulcer induced by indomethacin in rats. *Gen. Physiol. Biophys.* **2019**, *38*, 175.
(18) Denizalti, M.; Durlu-Kandilci, N. T.; Simsek, G.; Bozkurt, T. E.; Sahin-Erdemli, I. Rho kinase and protein kinase C pathways are responsible for enhanced carbachol contraction in permeabilized detrusor in a rat model of cystitis. *Basic Clin. Pharmacol. Toxicol.* **2018**, *123*, 567−576.
(19) Shabbir, R.; Hayat Malik, M. N.; Zaib, M.; Jahan, S.; Khan, M. T. Amino Acid Conjugates of 2-Mercaptobenzimidazole Ameliorates High-Fat Diet-Induced Hyperlipidemia in Rats via Attenuation of HMGCR, APOB, and PCSK9. *ACS Omega* **2022**, *7*, 40502−40511.
(20) Liu, Q.; Wu, Z.; Liu, Y.; Chen, L.; Zhao, H.; Guo, H.; Zhu, K.; Wang, W.; Chen, S.; Zhou, N.; Li, Y.; Shi, B. Cannabinoid receptor 2 activation decreases severity of cyclophosphamide-induced cystitis via regulating autophagy. *Neurourol. Urodyn.* **2020**, *39*, 158−169.
(21) Boeira, V. T.; Leite, C. E.; Santos, A. A.; Edelweiss, M. I.; Calixto, J. B.; Campos, M. M.; Morrone, F. B. Effects of the hydroalcoholic extract of Phyllanthus niruri and its isolated compounds on cyclophosphamide-induced hemorrhagic cystitis in mouse. *Naunyn-Schmiedeberg's Arch. Pharmacol.* **2011**, *384*, 265−275.
(22) Vieira, M. M.; Macêdo, F. Y. B.; Filho, J. N. B.; Costa, A. C. L.; Cunha, A. N.; Silveira, E. R.; Brito, G. A. C.; Ribeiro, R. A. Ternatin, a flavonoid, prevents cyclophosphamide and ifosfamide-induced hemorrhagic cystitis in rats. *Phytother. Res.* **2004**, *1*, 135−141.
(23) Mota, J. M.; Brito, G. A.; Loiola, R. T.; Cunha, F. Q.; Ribeiro, R. D. A. Interleukin-11 attenuates ifosfamide-induced hemorrhagic cystitis. *Int. Braz. J.* **2007**, *33*, 704−710.
(24) Hosny, M.; Eltaweil, A. S.; Mostafa, M.; El-Badry, Y. A.; Hussein, E. E.; Omer, A. M.; Fawzy, M. Facile synthesis of gold nanoparticles for anticancer, antioxidant applications, and photocatalytic degradation of toxic organic pollutants. *ACS Omega* **2022**, *7*, 3121−3133.
(25) Adesanwo, J. K.; Makinde, O. O.; Obafemi, C. A. Phytochemical analysis and antioxidant activity of methanol extract and betulinic acid isolated from the roots of Tetracera potatoria. *J. Pharm. Res.* **2013**, *6*, 903−907.
(26) Smaldone, M. C.; Vodovotz, Y.; Tyagi, V.; Barclay, D.; Philips, B. J.; Yoshimura, N.; Tyagi, P. Multiplex analysis of urinary cytokine levels in rat model of cyclophosphamide-induced cystitis. *Urology* **2009**, *73*, 421−426.
(27) Ho, D. R.; Chen, C. S.; Lin, W. Y.; Chang, P. J.; Huang, Y. C. Effect of hyaluronic acid on urine nerve growth factor in cyclophosphamide-induced cystitis. *Int. J. Urol.* **2011**, *18*, 525−531.
(28) O'Boyle, N. M.; Banck, M.; James, C. A.; Morley, C.; Vandermeersch, T.; Hutchison, G. R. Open Babel: An open chemical toolbox. *J. Cheminf.* **2011**, *3*, 33.
(29) Najm, S.; Naureen, H.; Sultana, K.; Anwar, F.; Rehman, S.; Arshad, S.; Khan, M. M. In-silico computational analysis of [6-(2, 3-Dichlorophenyl)-1, 2, 4-Triazine-3, 5-Diamine] metal complexes on voltage gated sodium channel and dihydrofolate reductase enzyme. *Pak. J. Pharm. Sci.* **2020**, *33*, 1779−1786.
(30) Yang, J.; Roy, A.; Zhang, Y. Protein−ligand binding site recognition using complementary binding-specific substructure comparison and sequence profile alignment. *Bioinformatics* **2013**, *29*, 2588−2595.
(31) Ebrahimipour, S. Y.; Sheikhshoaie, I.; Castro, J.; Dušek, M.; Tohidiyan, Z.; Eigner, V.; Khaleghi, M. Synthesis, spectral characterization, structural studies, molecular docking and antimicrobial evaluation of new dioxidouranium (VI) complexes incorporating tetradentate N 2 O 2 Schiff base ligands. *RSC Adv.* **2015**, *5*, 95104−95117.
(32) Mahmoud, W. H.; Deghadi, R. G.; Mohamed, G. G. Metal complexes of ferrocenyl-substituted Schiff base: Preparation, characterization, molecular structure, molecular docking studies, and biological investigation. *J. Organomet. Chem.* **2020**, *917*, No. 121113.
(33) Shrinivasan, M.; Skariyachan, S.; Aparna, V.; Kolte, V. R. Homology modelling of CB1 receptor and selection of potential inhibitor against Obesity. *Bioinformation* **2012**, *8*, 523.
(34) Kullmann, F. A.; Daugherty, S. L.; de Groat, W. C.; Birder, L. A. Bladder smooth muscle strip contractility as a method to evaluate lower urinary tract pharmacology. *J. Vis. Exp.* **2014**, No. e51807.
(35) Zhang, H.; Zhao, J.; Lu, Q.; Sun, B.; Liu, X.; Yang, C.; Li, S.; Li, L.; Yi, S.; Yang, Z.; Xu, J. Luteolin improves cyclophosphamide-induced cystitis through TXNIP/NLRP3 and NF-κB pathways. *Evidence-Based Complementary Altern. Med.* **2021**, *2021*, No. 1718709.
(36) Matz, E. L.; Hsieh, M. H. Review of advances in uroprotective agents for cyclophosphamide-and ifosfamide-induced hemorrhagic cystitis. *Urology* **2017**, *100*, 16−19.
(37) Mansour, D. F.; Salama, A. A.; Hegazy, R. R.; Omara, E. A.; Nada, S. A. Whey protein isolate protects against cyclophosphamide-induced acute liver and kidney damage in rats. *J. Appl. Pharm. Sci.* **2017**, *7*, 111−120.
(38) Nyathi, B.; Bvunzawabaya, J. T.; Mudawarima, C. V. P.; Manzombe, E.; Tsotsoro, K.; Selemani, M. A.; Munyuki, G.; Rwere, F. Antidiabetic and in silico molecular docking of Xeroderris stuhlmannii (Taub.) Mendonca & EP Sousa phytochemical compounds on human α-glucosidases. *bioRxiv*, **2022**. 2022−09.
(39) Rana, S.; Dixit, S.; Mittal, A. In silico target identification and validation for antioxidant and anti-inflammatory activity of selective phytochemicals. *Braz. Arch. Biol. Technol.* **2019**, 62.
(40) Yende, S. R.; Shah, S. K.; Arora, S. K.; Moharir, K. S.; Lohiya, G. K. In silico prediction of phytoconstituents from Ehretia laevis targeting TNF-α in arthritis. *Digital Chin. Med.* **2021**, *4*, 180−190.
(41) Zahran, E. M.; Abdel-Maqsoud, N. M. R.; Tammam, O. Y.; Abdel-Rahman, I. M.; Elrehany, M. A.; Bakhsh, H. T.; Altemani, F. H.; Algehainy, N. A.; Alzubaidi, M. A.; Abdelmohsen, U. R.; Elmaidomy, A. H. Scabicidal Potential of Coconut Seed Extract in Rabbits via Downregulating Inflammatory/Immune Cross Talk: A Comprehensive Phytochemical/GC-MS and In Silico Proof. *Antibiotics* **2023**, *12*, 43.
(42) Rahman, M. H.; Biswas, P.; Dey, D.; Hannan, M. A.; Sahabuddin, M.; Araf, Y.; Kwon, Y.; Emran, T. B.; Ali, M. S.; Uddin, M. J. An In-Silico Identification of Potential Flavonoids against Kidney Fibrosis Targeting TGFβR-1. *Life* **2022**, *12*, 1764.
(43) Gore, P. R.; Prajapati, C. P.; Mahajan, U. B.; Goyal, S. N.; Belemkar, S.; Ojha, S.; Patil, C. R. Protective effect of thymoquinone against cyclophosphamide-induced hemorrhagic cystitis through inhibiting DNA damage and upregulation of Nrf2 expression. *Int. J. Biol. Sci.* **2016**, *12*, 944.
(44) Martins, J. P.; Silva, R. B. M.; Coutinho-Silva, R.; Takiya, C. M.; Battastini, A. M. O.; Morrone, F. B.; Campos, M. M. The role of P2X7 purinergic receptors in inflammatory and nociceptive changes accompanying cyclophosphamide-induced haemorrhagic cystitis in mice. *Br. J. Pharmacol.* **2012**, *165*, 183−196.
(45) Giglio, D.; Ryberg, A. T.; Delbro, D. S.; Tobin, G. Altered muscarinic receptor subtype expression and functional responses in cyclophosphamide induced cystitis in rats. *Auton. Neurosci.* **2005**, *122*, 9−20.
(46) Dela Pena, I. C.; Yoon, S. Y.; Kim, S. M.; Lee, G. S.; Ryu, J. H.; Park, C. S.; Kim, Y. C.; Cheong, J. H. Bladder-relaxant properties of the novel benzofuroindole analogue LDD175. *Pharmacology* **2009**, *83*, 367−378.
(47) Kishii, K. I.; Hisayama, T.; Takayanagi, I. Comparison of contractile mechanisms by carbachol and ATP in detrusor strips of rabbit urinary bladder. *Jpn. J. Clin. Pharmacol.* **1992**, *58*, 219−229.
(48) Nagase, K.; Akino, H.; Yokokawa, R.; Ishida, H., Yokoyama, O. *73 The influence of the mucosa and bladder outlet obstruction on the effect of the cyclooxygenase inhibitor, indomethacin, on spontaneous contractile activity in the rat bladder*, 2013.
(49) Saima; Anjum, I.; Mobashar, A.; Jahan, S.; Najm, S.; Nafidi, H.-A.; Bin Jardan, Y. A.; Bourhia, M. Spasmolytic and Uroprotective Effects of Apigenin by Downregulation of TGF-β and iNOS Pathways and Upregulation of Antioxidant Mechanisms: In Vitro and In Silico Analysis. *Pharmaceuticals* **2023**, *16*, 811.

https://doi.org/10.1021/acsomega.3c01450
ACS Omega 2023, 8, 28196−28206